13. Miller, G. S. The families and genera of bats. *Bull. US Natl Mus.* **57,** 1–282 (1907).
14. Novacek, M. J. & Wyss, A. R. Higher-level relationships of the recent eutherian orders: morphological evidence. *Cladistics* **2,** 257–287 (1986).
15. Beard, K. C. in *Primates and their relatives in phylogenetic perspective* (ed. MacPhee, R. D. E.) 63–90 (Plenum, New York, 1993).
16. Rayner, J. M. V. The cost of being a bat. *Nature* **350,** 383–384 (1991).
17. Gould, E. Evidence for echolocation in the Tenrecidae of Madagascar. *Proc. Am. Phil. Soc.* **109,** 352–360 (1965).
18. Tomasi, T. E. Echolocation by the short-tailed shrew *Blarina brevicauda*. *J. Mammal.* **60,** 751–759 (1979).
19. Forsman, K. A. & Malmquist, M. G. Evidence for echolocation in the common shrew, *Sorex araneus*. *J. Zool. Lond.* **216,** 655–662 (1988).
20. Speakman, J. R & Racey P. A. No cost of echolocation for bats in flight. *Nature* **350,** 421–423 (1991).
21. Kalko, E. K. V. Coupling of sound emission and wing-beat in naturally foraging European pipistrelle (*Microchiroptera: Vespertilionidae*). *Folia Zool.* **43,** 363–376 (1994).
22. Springer, M. S. *et al.* Endemic African mammals shake the phylogenetic tree. *Nature* **388,** 61–64 (1997).
23. Stanhope, M. J. *et al.* Molecular evidence for multiple origins of Insectivora and for a new order of endemic African insectivore mammals. *Proc. Natl Acad. Sci. USA* **95,** 9967–9972 (1998).
24. Kishino, H. & Hasegawa, M. Evaluation of the maximum likelihood estimate of the evolutionary tree topologies from DNA sequence data, and the branching order within Hominoidea. *J. Mol. Evol.* **29,** 170–179.
25. Templeton, A. R. Phylogenetic inference from restriction endonuclease cleavage site maps with particular reference to the evolution of humans and the apes. *Evolution* **37,** 221–244 (1983).
26. Lyons-Weiler, J., Hoelzer, G. A. & Tausch, R. J. Relative Apparent Synapomorphy Analysis (RASA) I: the statistical measurement of phylogenetic signal. *Mol. Biol. Evol.* **13,** 749–757 (1996).

Acknowledgements

This work was supported by grants from the Training and Mobility of Researchers programme of the European Commission to M.J.S., and the National Science Foundation to M.S.S.

Correspondence and requests for materials should be addressed to M.J.S. (e-mail: Michael_J_Stanhope@sbphrd.com) or M.S.S. (e-mail: mark.springer@ucr.edu).

Human cerebellar activity reflecting an acquired internal model of a new tool

Hiroshi Imamizu*, Satoru Miyauchi†, Tomoe Tamada*, Yuka Sasaki†‡, Ryousuke Takino§, Benno Pütz*‡, Toshinori Yoshioka* & Mitsuo Kawato*‖

** JST/ERATO Kawato Dynamic Brain Project, 2-2 Hikaridai, Seika-cho, Soraku-gun, Kyoto 619-0288, Japan*
† Communications Research Laboratory, 588-2, Iwaoka, Nishi-ku, Kobe, Hyogo 651-2401, Japan
§ Shiraume Gakuen College, 1-830, Ogawa-cho, Kodaira-shi, Tokyo 1878570, Japan
‖ ATR Human Information Processing Research Laboratories, 2-2 Hikaridai, Seika-cho, Soraku-gun, Kyoto 619-0288, Japan

Theories of motor control postulate that the brain uses internal models of the body to control movements accurately. Internal models are neural representations of how, for instance, the arm would respond to a neural command, given its current position and velocity[1–6]. Previous studies have shown that the cerebellar cortex can acquire internal models through motor learning[7–11]. Because the human cerebellum is involved in higher cognitive function[12–15] as well as in motor control, we propose a coherent computational theory in which the phylogenetically newer part of the cerebellum similarly acquires internal models of objects in the external world. While human subjects learned to use a new tool (a computer mouse with a novel rotational transformation), cerebellar activity was measured by functional magnetic resonance imaging. As predicted by our theory, two types of activity were observed. One was spread over wide areas of the cerebellum and was precisely proportional to the error signal that guides the acquisition of internal models during learning. The other was confined to the area near the posterior superior fissure and remained even after learning, when the error levels had been equalized, thus probably reflecting an acquired internal model of the new tool.

Most neuroimaging studies have found that the regional blood flow in the human cerebellum increases significantly at the beginning of learning for a new motor or cognitive task and decreases as the learning proceeds[16–19]. These results are often interpreted as meaning that the cerebellum is involved only in the early phase of learning and is not a memory site, that is, it does not store internal models. Here we present a different interpretation (see also ref. 15) based on our computational theory and experimental results.

Previous cerebellar learning theories[20–22] make no specific predictions about the activity of internal models (see Supplementary Information for details). We have proposed that multiple internal models exist and that they compete to learn new environments and tools[23]. During the learning, all of these multiple internal models receive a copy of the error signal and only one or a few learn the new transformation, thereby reducing the error signal and localizing the new activity to a distinct region of the cerebellum. The two types of

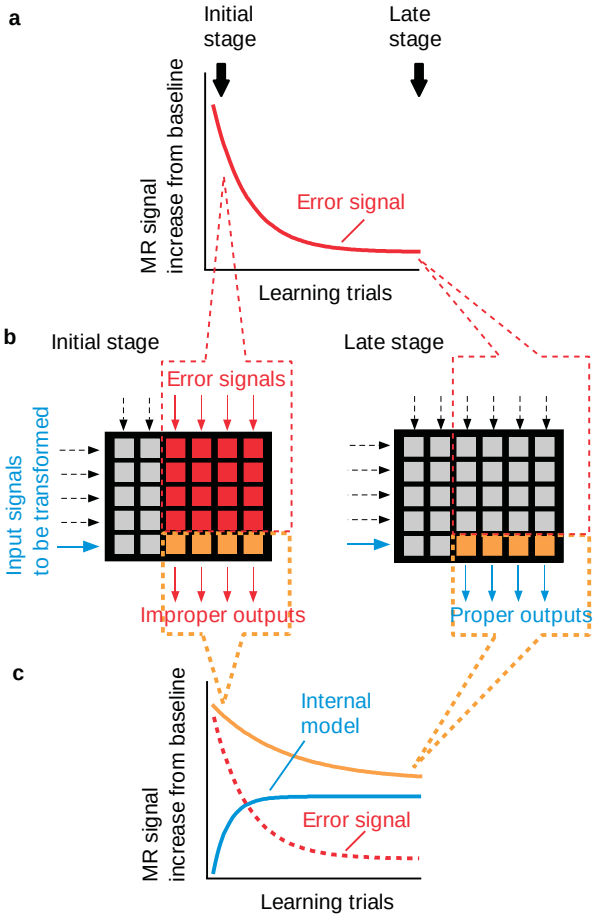

Figure 1 Changes in cerebellar activity predicted by the learning theory of internal models. **a**, Signal intensity change caused by error signals (red curve). **b**, Activity maps of the initial and late stages of learning. Each small square represents a unit of multiple internal models. Orange squares indicate regions where the internal model is acquired. **c**, Signal intensity change in the regions where the internal model is acquired. Orange curve indicates activity in the orange squares (the sum of activity reflecting error signals (red curve) and that reflecting the acquired internal model (cyan curve)).

‡ Present addresses: Massachusetts General Hospital NMR Center, 149, 13th Street, Charlestown, Massachusetts 02129, USA (Y.S.); Kernspintomographie, Max-Planck-Institut fur Psychiatrie, Kraepelinstrasse 10, 80804 Muenchen, Germany (B.P.).

cerebellar activity representing the error signals and the internal model are predicted to occur in specific spatio-temporal patterns (Fig. 1). Large error signals are fed into broad regions for all possible internal model candidates at the initial learning stage (red and orange in Fig. 1b). Because the subject's performance improves and the error signals decrease with learning, activity reflecting the error signals also decreases with learning (Fig. 1a). This prediction agrees with previous imaging data. However, signals representing the acquired internal model must increase (cyan curve in Fig. 1c) and remain even at the late stages of learning only in the limited region (orange in Fig. 1b). This region contains a group of the most accurate internal models. Even in this region, total activity is expected to decrease (orange curve in Fig. 1c) because the observed activity is the sum of the error signal (broken red curve) and the internal model (cyan curve). However, significant activity must remain even after the learning is complete. In our interpretation, the activity reflecting the learned model is smeared by the strong activity reflecting the error signal and, therefore, was not detected in previous imaging studies. In our present study, however, we found internal model activity by equalizing the errors under the baseline condition to those under the test condition. Furthermore, the time course of the internal-model activity (cyan curve in Fig. 1c) was estimated by subtracting the error signal activity (red curve) from the total activity (orange curve).

The task for the subjects was to manipulate a computer mouse so that the corresponding cursor followed a randomly moving target on a screen (Fig. 2a; a tracking task). Seven subjects performed the task for eleven sessions (training sessions). We used functional magnetic resonance imaging (fMRI) to scan the cerebellum in the odd-numbered sessions. Each session lasted 9 min and 23 s and comprised eight alternating blocks of test and baseline periods. During the test periods, the cursor appeared in a position rotated 120° around the centre of the screen to necessitate subject learning (novel mouse); during the baseline periods, it was not rotated (ordinary mouse). In the first session (Fig. 2b), large regions near the posterior superior fissure in the lateral cerebellum were significantly more active during the test periods than the baseline periods (correlation coefficient (CC) > 0.3); in the last session (Fig. 2c), only restricted subregions were activated. We confirmed that this activity cannot be attributed to larger hand movements (Fig. 2d) or larger eye movements in the test than in the baseline periods by showing that hand-movement or eye-movement activity is different from the activity shown in Fig. 2b and c (see also Supplementary Information).

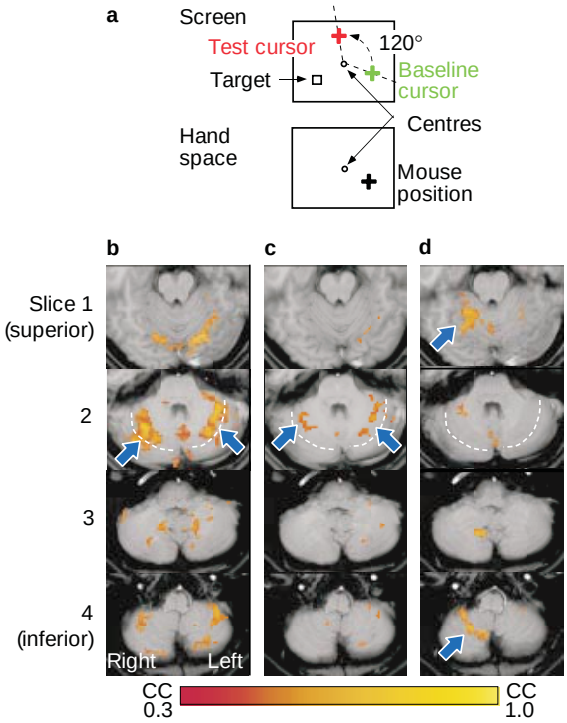

Figure 2 Visuomotor learning task and cerebellar activity. **a**, Rule for changing the relationship between mouse and cursor positions. A cross cursor coloured red or green appears on the screen in the test periods or baseline periods, respectively. The open circles indicate the centres of the screen and the hand space. **b**, Cerebellar activity of a typical subject in the first training session. The colour-coded regions were significantly activated in the test periods (CC > 0.3). The broken lines indicate the posterior superior fissure. **c**, Cerebellar activity of the same subject in the last training session. **d**, Regions that were more active during the tracking task (cursor position was not rotated) than during the task of pursuing the moving target with the eyes but without hand/mouse movements. These active regions are apparently different from those in **b** and **c** and are located in the superior anterior and inferior anterior parts of the cerebellum on the right side, ipsilateral to the hand that was performing the task.

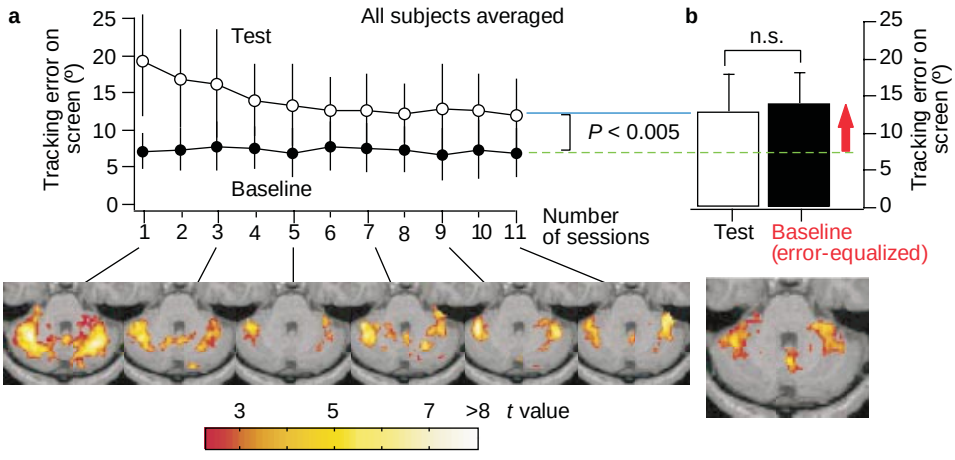

Figure 3 The two types of cerebellar activity. **a**, Activity that decreased with learning progress. Top, tracking error (mean ± s.d.) in the training sessions. Bottom, activation maps showing the regions that were significantly activated in the test periods in comparison to those in the baseline periods ($P < 0.05$ corrected). The slice position was approximately the same as slice 2 in Fig. 2. **b**, The activity that remained when the tracking error was equalized. Top, tracking error (mean ± s.d.) in the error-equalized session. n.s.: not significant ($F(1, 6) = 4.52$). Bottom, activation map.

The subjects' performances were measured by tracking errors (the distance between the cursor and the target; see Methods). The errors in the test periods decreased significantly as the number of sessions increased, whereas the errors in the baseline periods were constant (upper panel in Fig. 3a). A repeated-measures analysis of variance (ANOVA) on the errors indicated a significant effect of the sessions in the test periods ($F(10, 60) = 10.60$, $P < 0.001$) but no significant effect in the baseline periods ($F(10, 60) = 0.67$). Activation maps ($P < 0.05$, corrected for multiple comparisons) derived from data across all subjects (Fig. 3a) indicated that the activity in the lateral cerebellum became smaller as learning progressed (see Methods).

The learning during the test periods was sufficient for there to be no significant difference in the tracking error between any pairs of the last three sessions according to the *post hoc* test (at $P < 0.001$ level by Tukey's honestly significant difference method). Thus, the cerebellar activation observed in the late stage of learning should include the activity of the acquired internal model. However, we cannot conclude that the activation solely reflects the internal model because the test error was close to, but significantly larger than, the baseline error (for example, $F(1, 6) = 28.52$, $P < 0.005$ on the error in the last training session across all subjects). That is, the activation may partly reflect error signals.

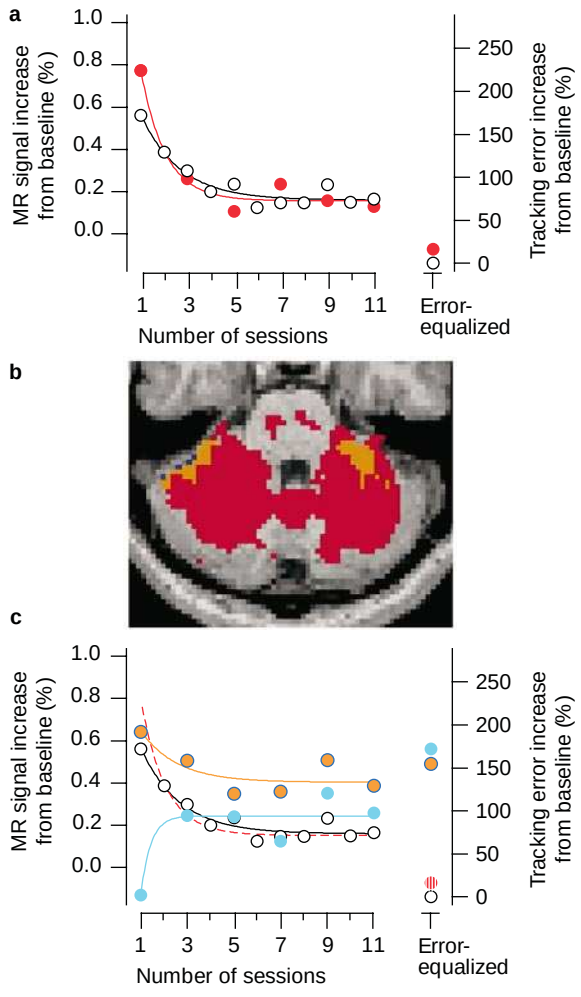

Figure 4 Cerebellar activity related to error signals and activity related to the acquired internal model. **a**, Activity change (red circles) in the red and orange regions in **b** in comparison to the decrease in tracking error (black circles). Each curve indicates the exponential function fitted to the circles. **b**, Activity in the red and orange regions was significantly ($P < 0.05$) correlated with the tracking error in the training sessions. Activity in the blue and orange regions was correlated with a step function representing the internal-model activity in the error-equalized session. **c**, Activity change in the blue and orange regions (blue circle filled by orange). The cyan circle indicates the subtraction of the activity in the red region from that in the blue and orange regions. The black circles and solid curve indicate the tracking error increase (as in **a**). The red broken curve is a duplication of the red curve in **a**.

To evaluate this possibility, all of the subjects underwent an 'error-equalized' experiment: the target velocity in the baseline periods was increased so that the baseline error was equal to the test error. Here, we used the linear relationship between error and target velocity (see Methods). As result, there was no significant difference between the test and the baseline errors (Fig. 3b, top). However, regions near the posterior superior fissure were significantly more active during the test periods than during the baseline periods (Fig. 3b, bottom). This activity cannot be related to the tracking error. Moreover, the amount of mouse movement (measured by the cursor trajectory length) and the target velocity in the baseline periods were significantly larger than those in the test periods ($F(1, 6) = 38.16$, $P < 0.001$, on average 2.38-fold, and $F(1, 6) = 156.63$, $P < 0.001$, on average 2.71-fold, respectively). All of the subjects reported that more effort and attention were needed in the baseline periods than in the test periods. Thus, the significant activity increase in the test period cannot be attributed to the mouse/hand movements, the visual target velocity, attention or effort. The most plausible explanation is that the remaining activity in Fig. 3b reflects the acquired internal models, whereas the decrease in activity as learning progresses (Fig. 3a) may largely reflect the error signals.

To strengthen the above conclusion quantitatively, we examined the time courses of gross signal intensity during all sessions averaged over two regions of interest. First, the error-related region (red and orange in Fig. 4b) was defined as voxels whose signal intensity during all the training sessions was significantly and positively correlated with the tracking error (that is, the estimated regression coefficient was significantly larger than zero, $t(5276) > 2.33$, $P < 0.05$ corrected). Second, the internal-model-related region (blue and orange in Fig. 4b) was defined as voxels whose signal intensity during the error-equalized session was significantly and positively correlated with the explanatory variable which takes 1 in the test period scans and 0 in the baseline period scans, and thus represents internal-model activity ($t(874) > 2.33$, $P < 0.05$ corrected). Orange voxels were correlated with both the tracking error and the internal model activity. The error-related region is widely spread over the lateral cerebellum, whereas the internal model seems to be acquired only in the restricted subregions.

The relative activity in the red and orange regions (per cent of mean signal increase from the baseline periods, all subjects averaged) decreased as the session number increased (red curve in Fig. 4a) and was highly correlated with the tracking error (per cent of increase from the baseline) indicated by the black curve ($r^2 = 0.82$ for all sessions, $F(1, 5) = 22.87$, $P < 0.005$). In contrast, the activity in the blue and orange regions did not markedly decrease (orange curve in Fig. 4c), and its correlation with the error was low ($r^2 = 0.25$, $F(1, 5) = 1.68$). The signal increase in the blue and orange regions was significantly larger than that in the red and orange regions ($F(1, 6) = 7.38$, $P < 0.05$). These data indicate that the activity in the blue and orange regions may include components that cannot be explained solely by the error. The cyan curve in Fig. 4c shows the subtraction of the red curve from the orange curve, and represents the internal model activity according to our theory. This activity increased at the initial phase of learning and remained high even in the late learning stage where the error was equalized (Fig. 4c, right).

The acquired internal models in these experiments are expected to represent the altered relationship between the cursor movement and the mouse movement (forward and/or inverse kinematics models of the novel tool). We believe that these internal models were stored in different regions from those for an ordinary mouse, as no significant activity was observed near the posterior superior fissure when the subjects used an ordinary mouse in the test periods

and pursued the moving target with the eyes but without hand/mouse movements in the baseline periods (see Fig. 2d and Supplementary Information). According to an electrophysiological study in monkeys[24], regions near this fissure receive parallel fibre inputs from the premotor and parietal association cortex, and are thus suitable to represent kinematic models of tools. The bilateral activity (see ref. 25 for related bilateral activity) may indicate that activated regions acquire internal models for cognitive function independent of the ipsilateral correspondence between the motor apparatus and the cerebellum. Whereas previous neurophysiological experiments indicated that internal models for the motor apparatus are present in phylogenetically older parts of the cerebellum (such as the ventral paraflocculus, vermis and intermediate parts)[8–11], internal models of objects and tools in the external world seem to reside in newer parts. We further speculate that the cerebellum assists information processing in cerebral areas by providing general internal models of extended controlled objects in the external world such as concepts, symbols and languages. □

Methods

Task

The subjects moved a computer mouse (PocketEgg, Elecom) using the right hand while lying in an MRI scanner. Head movements were restrained by a bite bar. They used a tilted mirror to view a rear-projection screen outside the scanner. A colour projector (VPH-1272OJ LCD; Sony) controlled by a computer (PC-9821 AP2; NEC) displayed the target and the cursor on the screen. During the tracking task, a small white square target was presented on a dark background. The x and y components of the target path were each sums of sinusoids whose amplitude and frequency were pseudorandomly determined. The subjects moved a small cross-hair cursor on the screen with the mouse. The cursor position was sampled at 60 Hz. The distance between the cursor and the target at each sampling point was accumulated over 4.4 s (tracking error).

Subjects

Ten neurologically normal subjects (20–34 years of age; five females and five males) participated in the experiments. Each participant gave informed written consent. Seven of the subjects (five right-handed and two left-handed[26]) underwent the training sessions and the error-equalized experiment. The other three subjects (two right-handed and one left-handed) underwent the training sessions and control experiments. In the control experiments, we confirmed that the activity observed in the above seven subjects could not be attributed to differences in hand or eye movements (see Fig. 2d and Supplementary Information).

MRI acquisition

A 1.5-T MRI scanner (Magnetom Vision; Siemens) was used to obtain blood oxygen level-dependent contrast functional images. Images weighted with the apparent transverse relaxation time (T_2^*) were obtained with an echo-planar imaging sequence (repetition time (TR) 4.4 s, echo time (TE) 66 ms, flip angle (FA) 90°, field of view (FoV) 240 mm × 240 mm, matrix size 128 × 128). We selected ten axial slices (thickness 7 mm, slice gap 0.21 mm) encompassing the cerebellum. We scanned 128 functional images for each slice during one session. Anatomical images for these slices were obtained with a T_1 weighted sequence (TR 350 ms, TE 6 ms, FA 90°, FoV 240 mm × 240 mm, matrix size 256 × 256).

MRI analysis

Motion artefacts in all functional images were removed by using Automated Image Registration (AIR) version 3.0 (ref. 27). We used two approaches to analyse the functional images: a correlation analysis on a pixel-by-pixel basis[28] and an analysis based on the general linear model as implemented in SPM99b (Wellcome Department of Cognitive Neurology). Details of the correlation analysis have been reported in ref. 29. To analyse group data, functional images of each subject's cerebellum were stereotactically transformed to a standard template in SPM, and were smoothed with a gaussian kernel 4 mm full width at half maximum (FWHM). In the activation analyses shown in Fig. 3, condition-specific effects were estimated with the linear model with a boxcar wave form. Areas of significant change in brain activity were specified by linear contrasts of the condition-specific effects and determined using the t-statistics (SPM{t}). Results were thresholded at t-value 2.33. In assessing the statistical significance of each cluster, we corrected for multiple comparisons based on random gaussian field theory in terms of spatial extent and/or peak height ($P < 0.05$). Voxel time series were temporally smoothed with a gaussian filter (FWHM of 4 s). We used the effective degree of freedom adjusted for analysis of fMRI time-series[30]. In the activation analyses shown in Fig. 4b, the explanatory variable of main interest was either the tracking error or the internal model activity.

Equalization of the tracking error according to the relationship between the error and the target velocity

The subjects performed the tracking task under various target velocities for about 15 min. The cursor position was not rotated during this task. The averaged target velocity ($21.30° s^{-1}$) used in the training sessions was multiplied by a value ranging from 1.0 to 5.0 at intervals of 0.2. Therefore, the target moved at 21 different averaged velocities in random order. Then, the relationship was estimated linearly by the least-squares method. The effect of the velocity on the error was significant ($r^2 > 0.70$, $F(1, 19) > 45.27$, $P < 0.0001$) for each subject. When the cerebellar activity was scanned, the target velocity was increased in the baseline period using this relationship, so that the baseline error was equal to the mean error in the preceding test period.

Received 12 July; accepted 14 October 1999.

1. Kawato, M., Furukawa, K. & Suzuki, R. A hierarchical neural-network model for control and learning of voluntary movement. *Biol. Cybern.* **57,** 169–185 (1987).
2. Lackner, J. R. & Dizio, P. Rapid adaptation to Coriolis force perturbations of arm trajectory. *J. Neurophysiol.* **72,** 299–313 (1994).
3. Shadmehr, R. & Mussa-Ivaldi, F. A. Adaptive representation of dynamics during learning of a motor task. *J. Neurosci.* **14,** 3208–3224 (1994).
4. Wolpert, D. M., Ghahramani, Z. & Jordan, M. I. An internal model for sensorimotor integration. *Science* **269,** 1880–1882 (1995).
5. Imamizu, H., Uno, Y. & Kawato, M. Internal representations of the motor apparatus: implications from generalization in visuomotor learning. *J. Exp. Psychol. Hum. Percept. Perform.* **21,** 1174–1198 (1995).
6. Gomi, H. & Kawato, M. Equilibrium-point control hypothesis examined by measured arm stiffness during multijoint movement. *Science* **272,** 117–120 (1996).
7. Kawato, M. & Gomi, H. A computational model of four regions of the cerebellum based on feedback-error learning. *Biol. Cybern.* **68,** 95–103 (1992).
8. Shidara, M., Kawano, K., Gomi, H. & Kawato, M. Inverse-dynamics model of eye movement control by Purkinje cells in the cerebellum. *Nature* **365,** 50–52 (1993).
9. Gomi, H. *et al.* Temporal firing patterns of Purkinje cells in the cerebellar ventral paraflocculus during ocular following responses in monkeys I. Simple spikes. *J. Neurophysiol.* **80,** 818–831 (1998).
10. Kobayashi, Y. *et al.* Temporal firing patterns of Purkinje cells in the cerebellar ventral paraflocculus during ocular following responses in monkeys II. Complex spikes. *J. Neurophysiol.* **80,** 832–848 (1998).
11. Kitazawa, S., Kimura, T. & Yin, P. B. Cerebellar complex spikes encode both destinations and errors in arm movements. *Nature* **392,** 494–497 (1998).
12. Raichle, M. E. *et al.* Practice-related changes in human brain functional anatomy during nonmotor learning. *Cereb. Cortex* **4,** 8–26 (1994).
13. Kim, S. G., Ugurbil, K. & Strick, P. L. Activation of a cerebellar output nucleus during cognitive processing. *Science* **265,** 949–951 (1994).
14. Allen, G., Buxton, R. B., Wong, E. C. & Courchesne, E. Attentional activation of the cerebellum independent of motor involvement. *Science* **275,** 1940–1943 (1997).
15. Thach, W. T. On the specific role of the cerebellum in motor learning and cognition: Clues from PET activation and lesion studies in man. *Behav. Brain Sci.* **19,** 411–431 (1996).
16. Friston, K. J., Frith, C. D., Passingham, R. E., Liddle, P. F. & Frackowiak, R. S. Motor practice and neurophysiological adaptation in the cerebellum: a positron tomography study. *Proc. R. Soc. Lond. B Biol. Sci.* **248,** 223–228 (1992).
17. Grafton, S. T., Woods, R. P. & Tyszka, M. Functional imaging of procedural motor learning: relating cerebral blood flow with individual subject performance. *Hum. Brain Mapp.* **1,** 221–234 (1994).
18. Seitz, R. J. *et al.* Successive roles of the cerebellum and premotor cortices in trajectorial learning. *NeuroReport* **5,** 2541–2544 (1994).
19. Flament, D., Ellermann, J. M., Kim, S. G., Ugurbil, K. & Ebner, T. J. Functional magnetic resonance imaging of cerebellar activation during the learning of a visuomotor dissociation task. *Hum. Brain Mapp.* **4,** 210–226 (1996).
20. Marr, D. A theory of cerebellar cortex. *J. Physiol. (Lond.)* **202,** 437–470 (1969).
21. Albus, J. S. A theory of cerebellar function. *Math. Biosci.* **10,** 25–61 (1971).
22. Ito, M. Cerebellar control of the vestibulo-ocular reflex—around the flocculus hypothesis. *Annu. Rev. Neurosci.* **5,** 275–296 (1982).
23. Wolpert, D. M. & Kawato, M. Multiple paired forward and inverse models for motor control. *Neural Netw.* **11,** 1317–1329 (1998).
24. Sasaki, K. *et al.* Mossy fibre and climbing fibre responses produced in the cerebellar cortex by stimulation of the cerebral cortex in monkeys. *Exp. Brain Res.* **29,** 419–428 (1977).
25. Roland, P. E., Eriksson, L., Widen, L. & Stone-Elander, S. Changes in regional cerebral oxidative metabolism induced by tactile learning and recognition in man. *Eur. J. Neurosci.* **1,** 3–18 (1988).
26. Oldfield, R. C. The assessment and analysis of handedness: the Edinburgh inventory. *Neuropsychologia* **9,** 97–113 (1971).
27. Woods, R. P., Grafton, S. T., Holmes, C. J., Cherry, S. R. & Mazziotta, J. C. Automated image registration: I. General methods and intrasubject, intramodality validation. *J. Comput. Assist. Tomogr.* **22,** 139–152 (1998).
28. Bandettini, P. A., Jesmanowicz, A., Wong, E. C. & Hyde, J. S. Processing strategies for time-course data sets in functional MRI of the human brain. *Magn. Reson. Med.* **30,** 161–173 (1993).
29. Tamada, T., Miyauchi, S., Imamizu, H., Yoshioka, T. & Kawato, M. Cerebro-cerebellar functional connectivity revealed by the laterality index in tool-use learning. *NeuroReport* **10,** 325–331 (1999).
30. Worsley, K. J. & Friston, K. J. Analysis of fMRI time-series revisited—again. *Neuroimage* **2,** 173–181 (1995).

Supplementary information is available on *Nature*'s World-Wide Web site (http://www.nature.com) or as paper copy from the London editorial offices of *Nature*.

Acknowledgements

We thank D. Wolpert, C. Miall, M. Honda, K. Sakai and S. Kitazawa for comments on the manuscript. Supported by Human Frontier Science Projects, and Special Coordination Fund to Brain Science.

Correspondence and requests for materials should be addressed to H.I. (e-mail: imamizu@erato.atr.co.jp).